Design and calibration process of solar sensors for small satellite missions

Angel Porras-Hermoso[1], *Daniel Alfonso-Corcuera, Javier Piqueras, Elena Roibás-Millán, Javier Cubas, Javier Pérez-Álvarez, Santiago Pindado*

Abstract
In combination with magnetometers, solar sensors are one of the most used instruments for determining the attitude of small satellites. These devices use the photoelectric effect to produce an electrical current. This electrical current, or the voltage associated with the electrical circuit of the solar sensor, is measured in order to compute the angle of incident of the sun with the normal direction of the sensor. Then, together with the computed angles of other solar sensors on different faces of the satellite, the sun's direction in relation to a spacecraft can be calculated. Solar sensors are simple devices whose low-cost design based on photodiodes can be developed by students. During the design and fabrication process of a solar sensor, one of the most important tasks is the accurate estimation of the sensor response in the space radiative environment. It is possible to simulate the Sun's radiation spectrum, but the equipment and facilities needed are costly for a university project. In this paper, the design and calibration process of satellite solar sensors carried out together by students and teachers from the Master's degree in Space Systems (MUSE) from the *Universidad Politécnica de Madrid* is described. The process uses a calibration method that calibrates the photodiodes for space use without simulating the Sun's radiation spectrum in the laboratory.

Keywords
ADCS, UPMsat-2, master in space systems, photodiodes, solar sensors

[1] Corresponding author: Universidad Politécnica de Madrid, Instituto Universitario de Microgravedad "Ignacio Da Riva" (IDR/UPM), Spain, angel.porras.hermoso@upm.es

Nomenclature

α	*sun incidence angle*
λ	*Wavelength*
Φ_{eff}	*Effective radiant flux*
$V(\lambda)$	*Luxmeter spectral sensitivity*
κ	*Boltzmann's constant*
A_s	*Photodiode area*
a	*Ideality factor*
C_v	*Luxmeter constant*
E_λ	*Spectral irradiance*
$\hat{E}_\lambda$	*Normalized spectral irradiance*
I	*Current*
I_0	*Reverse saturation current*
I_{pv}	*Photovoltaic current*
M	*Linear fitting slope*
n	*Linear fitting offset*
K	*Irradiance magnitude*
P	*Conversion efficiency factor*
q	*Electron charge*
R_L	*Resistor*
R_s	*Series resistor*
R_{sh}	*Shunt resistor*
$\hat{S}_\lambda$	*Normalized sensitivity function*
T	*Temperature*
V	*Voltage*
V_T	*Thermal voltage*

Acronyms/Abbreviations

COTS	*Commercial off-the-shelf*
IDR/UPM	*Instituto Universitario de Microgravedad Ignacio Da Riva*
LEO	*Low Earth Orbit*
MUSE	*Master on Space Systems at UPM*
UPM	*Univesidad Politécnica de Madrid*

1. Introduction

The Master on Space Systems (*Máster Universitario en Sistemas Espaciales* - MUSE) at *Universidad Politécnica de Madrid* (UPM) is project-based learning oriented [1], as it is characterized by a significant amount of practical work by the students, directly linked to *Instituto Universitario de Microgravedad "Ignacio Da Riva"* (IDR/UPM) running space projects. This master's degree is designed to reduce as much as possible the initial training required by graduates once enrolled in a space engineering company. One of the most recent and successful examples of this philosophy is the UPMSat-2 [2].

The UPMSat-2 is a 50 kg microsatellite designed, developed, and tested at the IDR/UPM, that was launched in the VV16 VEGA mission in September 2020. This project transmitted a great impetus to MUSE involving several promotions of students in the design and validation of different subsystems of this spacecraft [3,4]. Moreover, the development of UPMSat-2 has also allowed students to participate in different research projects, as it proves the different works published in the main lines of research of the institute as Attitude Determination and Control Subsystems, thermal control subsystems, structural analysis, spacecraft power subsystems and spacecraft instrumentation, which is the topic of this work.

Sun sensors are instruments responsive to a light source. With the information provided with these sensors, the relative orientation of the satellite in relation to the Sun is calculated. Given the simplicity, low cost, and low weight of these sensors, it is easy to understand why they are widely used, in combination with magnetometers, in small spacecraft for attitude determination [5,6].

In the present work, a simple way to test, calibrate, and operate a solar sensor based on COTS components is described. The selection and placement of the photodiodes plays an important role in the performance of the system, but if an accurate measure of the Sun vector is desired, it is necessary to calibrate each one of the photodiodes to characterize their specific response curve. This process, in appearance easy, can become complicated, especially if specialized equipment is missing. Both students and professors of MUSE faced this problem of characterizing the expected response of the photodiodes in space. The solar spectrum reaching Earth (AM 1.5) is not the same as the one received in space (AM0). Most of the photodiode calibration techniques found in the literature [7–9] are based on the simulation of the AM0 spectrum, but this requires specific instrumentation, which is usually costly for a university project. Fortunately, it is possible to characterize the in-flight performance of the photodiode if the photodiode is tested with a source of light whose spectrum is known. In this work, a simple process to calibrate photodiodes without requiring any specialized instrumentation is described.

2. Sun sensor electrical design

The Sun sensor developed for the UPMSat-2 consists of a total of six OSRAM BPX61 photodiodes [10], each facing one of the main positive and negative axes (±*X*, ±*Y*, ±*Z*) of the satellite. The photodiodes are connected to a 5 V power line from the power distribution unit and a resistance R_L (see Figure 1.A). The voltage drop across the resistance is recorded by the computer. Each photodiode voltage is compared to the maximum expected response of the photodiode, and the sun direction is derived. Regarding the selection of *RL,* as it is desirable to work near the short-circuit point of the photodiode, where the behaviour is more linear, the value of R_L should be small (in this case, a 32 Ω resistor was selected).

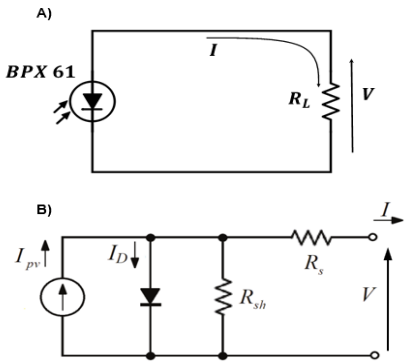

Figure 1. A) Sketch of the electric circuit to read the voltage response of the photodiodes. B) 1-Diode/2-resistor equivalent circuit model.

To select a correct value for the resistance and know its expected response in space, it is necessary to have a model that approximates the electrical behaviour of the photodiode. In this case, the equivalent circuit model of a 1 diode / 2 resistor (see Figure 1.B) is implicitly correlated with the output current with the photodiode voltage by the following equation:

$$I = I_{pv} - I_0\left[\exp\left(\frac{V+IR_s}{aV_T}\right)-1\right]-\frac{V+IR_s}{R_{sh}}, \quad (1)$$

where the thermal voltage, V_T, is defined as follows:

$$V_T = \frac{\kappa T}{q}. \quad (2)$$

The 1-Diode/2-resistor equivalent circuit described in Eq. (1) contains five parameters I_{pv}, I_0, *a*, R_{sh}, and R_s, that must be adjusted with the experimental data. Testing set-up and methodology

To fully characterize the photodiode response with the instrumentation available at an academic laboratory, two separate tests were performed. First, an illumination test was performed to measure the expected response of the photodiodes to the light they will receive in orbit. Second, an angular test was done to characterize the response of the photodiode when the angle between the normal of the sensor and the light source is changed.

2.1. Illumination test

The illumination test (see Figure 2) can be summarized as follows. The sensor is exposed to a light source with a known illuminance (red LED light for this case). The electrical circuit of Figure 1 is completed with a resistance. The output voltage and current shall be measured. Also, a luxmeter [11] placed near the photodiode is needed to measure the brightness of the light source.

Figure 2. Illumination test set-up.

Once the set-up is done, a correlation process is required to know the photodiode response to any source of light. The first step is to calculate the spectral irradiance that reaches the photodiode from the illuminance value given by the luxmeter. Eq. (3) provides the expression to calculate the illuminance provided by the luxmeter, as the photopic function is a normalized curve, a constant C_v = 683 lm/W is necessary to obtain the value in SI units.

$$E_v = C_v\int_\lambda V(\lambda)E_\lambda(\lambda)\,\mathrm{d}\lambda \quad (3)$$

$$E_\lambda(\lambda) = K\,\hat{E}_\lambda(\lambda) \quad (4)$$

Taking into account that the spectral irradiance can be expressed as the product of the normalized irradiance with a constant denoting its magnitude (Eq.4), the constant can be calculated as follows:

$$K = \frac{E_v}{C_v\int_\lambda V(\lambda)\hat{E}_\lambda(\lambda)\,\mathrm{d}\lambda}. \quad (5)$$

Then, the effective radiance flux that the sensor converts into current can be expressed as:

$$\Phi_{eff} = A_s K \int_\lambda \hat{S}_\lambda(\lambda)\hat{E}_\lambda(\lambda)\mathrm{d}\lambda\,, \qquad (6)$$

where the normalized spectral sensitivity function of the sensor is provided by the manufacturer.

The next step in this process is to correlate the effective radiant power in the photodiode with the voltage response that is being measured. As the manufacturer provides the normalized sensitivity curve and its constant, the output current can be expressed as follows:

$$I_{pv} = S_\lambda \Phi_{eff} = P\int_\lambda \hat{S}_\lambda(\lambda)E_\lambda(\lambda)\mathrm{d}\lambda\,, \qquad (7)$$

where *P* is a new parameter defined as the product of the photodiode area and its spectral sensitivity constant. This new parameter can be seen as the conversion efficiency between the effective irradiance and the generated current. The manufacturer values of $\hat{S}_\lambda$, A_s and S_λ are typical values that allow the calculation of the photodiode response for any spectrum. However, these typical values do not represent the exact response of each photodiode. Therefore, the objective of the calibration process is to correctly characterise the parameter *P*, among the I_0, *a*, R_{sh}, and R_s parameters of the 1D/2R equivalent circuit. Ideally $\hat{S}_\lambda$ should also be characterized, but this would require specialized instrumentation, which was not available. The parameter *P* can replace the parameter I_{pv} with the following equation:

$$P = \frac{I_{pv}}{K\int_\lambda \hat{S}_\lambda(\lambda)\hat{E}_\lambda(\lambda)\mathrm{d}\lambda}\,. \qquad (8)$$

The advantage of using *P* is that it is an intrinsic characteristic of the photodiode that does not depend on the illuminance received, in contrast to I_{pv}. The calibration process can be seen as an optimization problem with five degrees of freedom. The proposed objective function to minimize is the root mean square error (RMSE) between the model and experimental results:

$$\mathrm{RMSE} = \sqrt{\frac{1}{n}\sum_{i=1}^{n}\left(I_{i,exp} - I_{i,model}\right)^2}\,. \qquad (9)$$

The different experimental results are obtained by varying the resistor value connected to the photodiode. This process must be repeated for different illuminance conditions (a minimum of two sets of experiments should be done considering that the voltage response grows linearly with the illuminance near the short-circuit region). Therefore, once the illumination test has been done for different illumination conditions, it is possible to determinate the slope of $\mathrm{d}V_{\mathrm{exp}}/\mathrm{d}E_v^{\mathrm{LED}}$ through a linear fitting. Then considering that $\mathrm{d}I/\mathrm{d}E_{eff}$ is a constant of the photodiode, the relation between E_{eff} of the LED and the AM0 is known, and the values of the test resistance and flight resistance are also known, it is possible to calculate the the variation of the measured voltage with the solar irradiation as follows:

$$\frac{\mathrm{d}V_{\mathrm{flight}}}{\mathrm{d}E^{\mathrm{AM0}}} = \frac{\mathrm{d}V_{\mathrm{exp}}}{\mathrm{d}E_v^{\mathrm{LED}}}\frac{R_{\mathrm{flight}}}{R_{\mathrm{exp}}}\frac{E_v^{LED}\Phi_{eff}^{AM0}}{\Phi_{eff}^{LED}}\,. \qquad (10)$$

2.2. Angular test

The main idea of the angular test (see Figure 3) is to characterize the behavior of the photodiode when the relative angle between the sensor and the light source changes. It is common to approximate the angular response of the photodiode as the product of the cosine of the incidence angle measured from the normal direction of the sensor, and its maximum response the source of light reaching the photodiode. Although a cosine law is a good approach for most of the angular behaviour, this law lacks accuracy when there are high incidence angles between the normal of the sensor and the light source. Therefore, to obtain the maximum accuracy, it is necessary to calibrate the angular response of the photodiodes in their operative range.

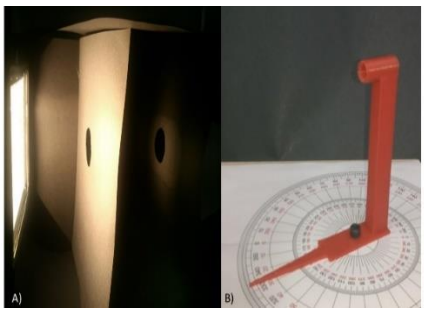

Figure 3. Angular test set-up.

3. Result and Discussion

3.1. Illumination test results

The results regarding the illumination test are presented graphically in Figure 4 where the *I-V* of the photodiode is obtained changing the value of the resistance connected to the sensor as noted for the resistance of 10 Ω and 50 Ω. In this figure, the results of the fitted model are

also plotted to compare the modelled results with the experimental data, showing good concordance between them. Finally, in Table 1 are shown the parameters of the fitted model for one of the photodiodes. It is interesting to note that the value obtained from the P parameter showed a significant deviation from the typical value provided by the manufacturer (P = $4.35 \cdot 10^{-6}$ Am²/W) which do not adequately represent the conversion efficiency.

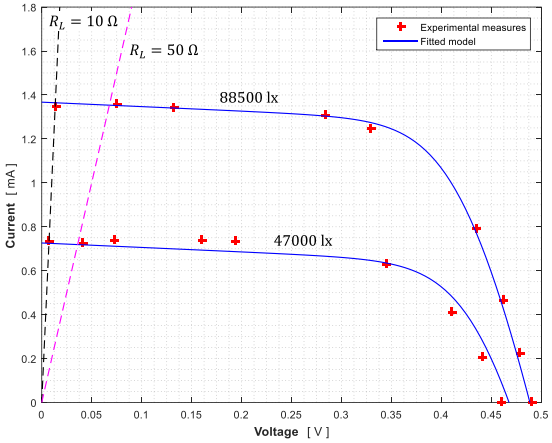

Figure 4. Results of the illuminaton testing campaign of one of the photodiodes and comparison with the fitted model.

Table 1. Value of the parameters extracted from the fitting process of the data from Figure 4.

Parameter	Fitted value
P [Am²/W]	$5.56 \cdot 10^{-6}$
I_0 [A]	$1 \cdot 10^{-10}$
a	1.1754
R_s [Ω]	34.01
R_{sh} [Ω]	4902

The results of the expected performance of the photodiodes in the AM0 spectrum for the Low Earth Orbit (LEO) are presented graphically in Figure 5. In the first graph, it is possible to observe how the experimental data present an almost perfect linear correlation between the measured voltage and the illuminance reaching the photodiodes. Then in Figure 5. B) the expected measurements for the AM0 spectrum in relation to the solar irradiance are presented. The information of this figure is completed with the coefficients calculated for each light source (See Table 2).

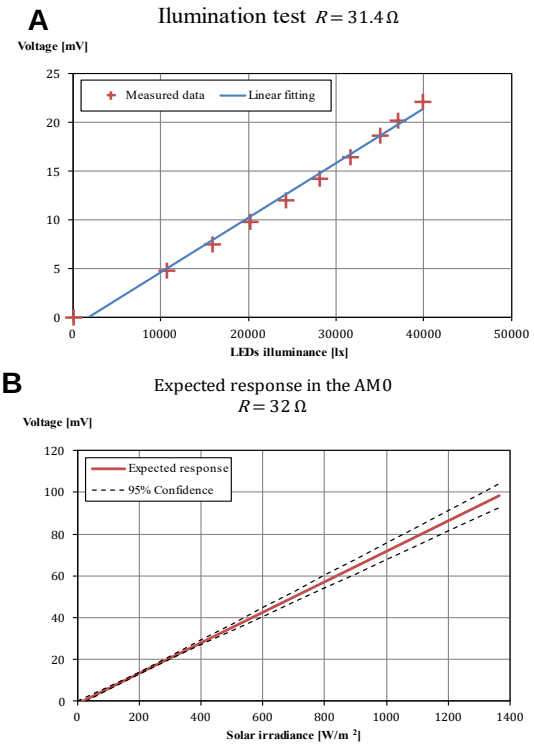

Figure 5. A) Fitting of the photodiode in relation to the illuminance. B) Expected response of the sensor to the AM0 spectrum irradiance.

Table 2. Coefficients obtained from the linear fitting of the results plotted in Figure 5.

Irradiance	*M*	*n* [mV]
LED	$5.59 \cdot 10^{-4}$ mV/lx	–0.992
AM0	$7.27 \cdot 10^{-2}$ mV/(W/m²)	–1.01

3.2. Angular test results

The results of the angular test are represented graphically in Figure 6. In the first graph, the normalized experimental results with a halogen source of light are represented. Then in the second graph it is represented the relative incidence angle between the normal direction of the photodiode and the source of light in relation to the measured voltage. It is important to note that the incidence angles in bracket [0° - 45°] show a distribution that resembles a cosine function. However, for angles larger than 45° this approximation starts to lack of accuracy. Therefore, instead of a cosine law, a 7th degree polynomial was used:

$$\alpha = b_0 + \sum_{n=1}^{7} b_n \left(\frac{V}{V_{\max}} \right)^n . \qquad (11)$$

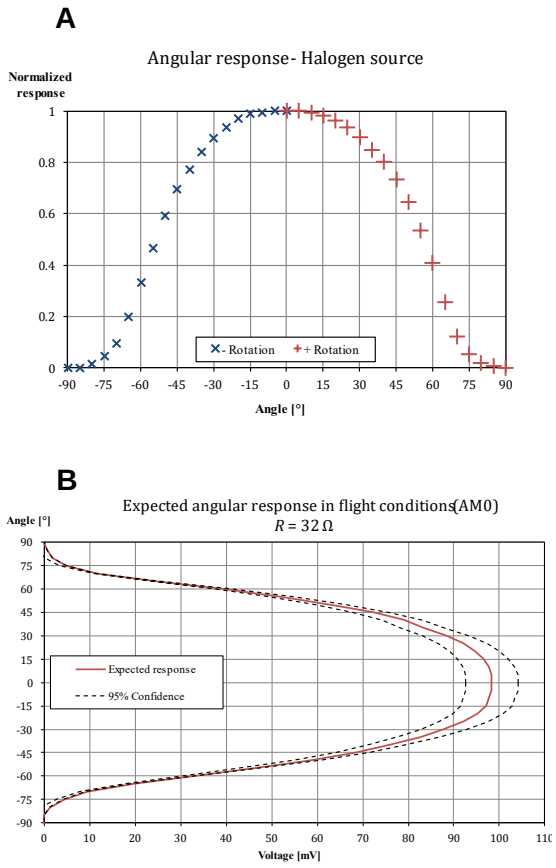

Figure 6. A) results from the angular test. B) Expected angular response of the photodiode in AM0 spectrum for LEO conditions.

4. Conclusions

The proposed methodology allows the calibration and determination of the expected performance of photodiodes in the direct polarization zone for any light spectrum without requiring any specialized equipment. This methodology was applied to the photodiodes of the Sun sensors of the UPMSat-2, resulting in a successful calibration of the photodiodes to LEO environment. Besides, it allowed a quite accurate estimation of this spacecraft attitude within its orbit. Additionally, the Sun sensors can be combined with data from solar panels to improve the accuracy of the attitude estimation.

Acknowledgements

This research has been partially supported by the project 478 Y2020/NMT-6427 OAPES from the program "Sinérgicos 2020" from *Comunidad de Madrid* (Spain). The authors are indebted to the Horizon 2020 IOD/IOV Programme of the European Union that funded the UPMSat-2 launch.

References

[1] S. Pindado et al., MUSE (Master in Space Systems), an Advanced Master ' s Degree in Space Engineering, in: ATINER'S Conf. Pap. Ser., 2016: pp. 1–16.

[2] S. Pindado et al., The UPMSat-2 Satellite : An Academic Project within Aerospace Engineering Education, in: ATINER'S Conf. Pap. Ser. No ENGEDU2017-2333, 2017: pp. 1–28. www.atiner.gr/papers.htm.

[3] J.M. Álvarez-Romero et al., UPMSat-2 Communications System Design , Integration and Testing , within MUSE (Master in Space System), in: ATINER's Conf. Pap. Proc. Ser. ENGEDU2019-0177, Athens, Greece, 2020: pp. 1–24.

[4] J.M. Álvarez-Romero et al., Research-Based Learning : Projects of Educational Innovation within MUSE (Master on Space Systems), in: ATINER ' s Conf. Pap. Proc. Ser., Athens, Greece, 2020: pp. 1–20.

[5] H. Abdelwahab et al., Maximizing solar energy input for Cubesat using sun tracking system and a maximum power point tracking, Proc. - 2017 Int. Conf. Commun. Control. Comput. Electron. Eng. ICCCCEE 2017. (2017)..

[6] D.J. Richie et al., Photocells for Small Satellite, Single-axis Attitude Determination, JoSS. 4 (2015) 285–299.

[7] J.C. Springmann, Satellite Attitude Determination with Low-Cost Sensors, (n.d.).

[8] H.R. Haave et al., Simulating Sun Vector Estimation and Finding Gyroscopes for the NUTS Project, (n.d.).

[9] P. Ortega et al., A Miniaturized Two Axis Sun Sensor for Attitude Control of Nano-Satellites, IEEE Sens. J. 10 (2010) 1623. https://doi.org/10.1109/JSEN.2010.2047104.

[10] O. Electronics, OSRAM BPX61 Datasheet, (2012).

[11] D. Ohm, HD2102.2 Luxmeter Manualle, (2010).